Surface modified used rubber tyre aggregates: effect on recycled concrete performance

Su, Haolin; Yang, Jian; Ghataora, Gurmel; Dirar, Samir

DOI:
10.1680/macr.14.00255

SURFACE MODIFIED USED RUBBER TYRE AGGREGATES: EFFECT ON RECYCLED CONCRETE PERFORMANCE

Haolin Su[1], Jian Yang[1], Gurmel S. Ghataora[2], and Samir Dirar[2]

Abstract:

Although research has found that using rubber in concrete will enhance its resilience and reduce its density, the significant loss of strength owing to lack of bonding has remained unresolved. This study considers how to minimise the loss of strength of concrete with used rubber tyre crumb aggregates and investigates the improvement of water permeability resistance that may consequentially develop. A surface of rubber crumb was modified by soaking in the saturated sodium hydroxide solution or silane coupling agent (SCA) before using. Up to 20% of natural fine aggregate was volumetrically replaced with treated rubber crumb. Experimental results show higher compressive and flexural strengths, Young's modulus and water permeability resistance from the samples with SCA-treated rubber than with as-received or sodium-hydroxide-treated rubber. X-ray diffraction pattern analyses indicate almost no change in crystalline phase for the rubber surface modification. Microscopic inspections show an enhanced rubber-matrix adhesion with the use of SCA. Results of mercury intrusion porosimetry reveal that concrete with SCA-treated rubber has a similar pore size distribution to the other three mixes, but achieves the lowest porosity and highest tortuosity, resulting in the best water permeability resistance. A brief cost analysis suggests that this method of surface modification is economically viable.

[1] School of Naval Architecture, Ocean and Civil Engineering, Shanghai Jiao Tong University, Shanghai, People's Republic of China; also School of Civil Engineering, University of Birmingham, Birmingham, UK

[2] School of Civil Engineering, University of Birmingham, Birmingham, UK

Introduction

The rapid growth of vehicle use has resulted in a huge increase in waste tyres. This has created a pressing problem known as 'black pollution', which poses a potential threat to the environment and human health (Nehdi and Khan, 2001). These waste tyres may create fire hazards, and they occupy a large volume of decreasing landfill sites with components that are non-biodegradable (Raghavan et al., 1998). Several methods of recycling or reusing waste tyres have been proposed, including their use as lightweight aggregates in asphalt pavements, as fuel for cement kilns, as feedstock for making carbon black, and as artificial reefs in marine environments (Prasad et al., 2009; Raghavan et al., 1998). However, some of these proposals are economically and environmentally unviable.

Many studies have been carried out on the use of waste tyre rubber as aggregate substitutes for making concrete (Aiello and Leuzzi, 2010; Albano et al., 2005; Benazzouk et al., 2007; Bignozzi and Sandrolini, 2006; Eldin and Senouci, 1993; Ganjian et al., 2009; Guneyisi et al., 2004; Khaloo et al., 2008; Khatib and Bayomy, 1999; Li et al., 2004, 2009; Ling, 2011; Savas et al., 1997; Segre and Joekes, 2000; Siddique and Naik, 2004; Snelson et al., 2009; Tantala et al., 1996; Topçu, 1995; Topçu and Avcular, 1997; Toutanji, 1995; Yang et al., 2011a). Like recycled construction or demolition aggregate (Gokce and Simsek, 2013; Hansen and Narud, 1983; Poon et al., 2004; Ravindrajah et al., 2006; Saravanakumar and Dhinakaran, 2014; Singh et al., 2013; Yang et al., 2011b), recycled waste tyre rubber within concrete can be a feasible option for sustainable and eco-friendly construction. Although the existing literature has considered different aspects with regards to the properties of rubber concrete, the general consensus is that the use of crumb rubber as aggregate in concrete will reduce its workability and strength, but will improve its ductility, impact resistance and dynamic energy dissipation capacity, and this is attributed to the rubber aggregate's own properties of high resilience and low density. One of the most important influencing factors on the properties of rubber concrete is the rubber replacement percentage, which has been widely studied and reported (Aiello and Leuzzi, 2010;

Benazzouk et al., 2007; Bignozzi and Sandrolini, 2006; Eldin and Senouci, 1993; Ganjian et al., 2009; Guneyisi et al., 2004; Khaloo et al., 2008; Khatib and Bayomy, 1999; Li et al., 2009; Savas et al., 1997; Snelson et al., 2009; Topçu, 1995; Toutanji, 1995; Yang et al., 2011a). The decrease in concrete compressive strength with an increase of rubber content has been consistently reported, and how to reduce the loss of strength of rubber concrete is constantly being investigated. There has been some research studying the effect of rubber surface modification on the properties of concrete, but this area of investigation is limited. Segre and Joekes (2000) carried out surface treatment on rubber particles by stirring with saturated sodium hydroxide (NaOH) solution for 20 min at room temperature before the mixture was filtered, and the rubber was then washed with tap water and dried at the ambient temperature before using. The results showed that the sodium hydroxide treatment enhanced the adhesion of tyre rubber particles to the surrounding paste, leading to an improvement in mechanical properties such as compressive strength, flexural strength and fracture energy. In contrast, Albano et al. (2005) pointed out that prior treatment of rubber with sodium hydroxide did not produce obvious changes in the compressive and splitting tensile strength of the resulting concrete when compared to untreated rubber concrete.

In order to address the negative results of reduced strength that the rubber concrete has often led to, this study aims to explore the potential treatments of crumb rubber and the resulting effects on the concrete properties. To this end, four groups of rubber concrete samples were devised and a series of concrete properties tests were carried out to reveal the differences resulting from the various methods of surface treatment of rubber particles before they are added into the concrete mixture. All studied concrete samples include recycled coarse aggregate, in addition to the crumb rubber partially replacing the fine natural aggregate particles. Saturated sodium hydroxide solution and silane coupling agent (SCA) were both used to modify the surface of rubber particles. Tests on workability at the fresh stage, cube compressive strength, Young's modulus, flexural strength and water permeability at the hardened stage were conducted. The results obtained are expected to

provide a method to reduce the loss of strength and to improve the water permeability resistance of rubber concrete.

Experiment details

Materials

The materials used in this study comprised cement, tap water, sand, natural gravels, recycled aggregates and waste tyre rubber. Cement (CEM II/B-V 32.5) with 30% pulverised fuel ash (PFA) was used as a binder for the concrete mixture. Natural river sand having a nominal maximum particle size (NMPS) of 5 mm was used as fine aggregate. Washed crushed gravels with a NMPS of 10 mm were used as coarse aggregate. Recycled aggregates from a local demolition plant, with the same NMPS, were used to replace 50% of natural coarse aggregates by mass for all four concrete mixes. Figure 1 shows the typical composition of recycled concrete aggregates. Combined size rubber (CSR) with continuous grading (blending different sized rubber particles artificially), similar to natural sand (shown in Figure 2), was sourced from the local recycling industry to replace 20% of sand by volume. Saturated sodium hydroxide solution and SCA were prepared to modify the surface of the rubber particles. Two batches of rubber particles were soaked in saturated sodium hydroxide solution for 2 h and 24 h, respectively, under ambient conditions. They were then washed with tap water and kept in laboratory condition for 24 h before using. Another batch was soaked in SCA until the entire surface was coated by the agent before being added into the mixture.

Mix design

The British Department of the Environment (DoE) method that is widely used for concrete mix design in the UK was adopted in this study. The saturated surface dry (SSD) density and SSD water absorption of the aggregates and crumb rubber are shown in Table 1. The mix design of the control concrete aimed to achieve a target mean strength (grade C30/37) of 43

MPa at 28 d with a slump value of 60–180 mm. In total, four concrete mixes were prepared: the control mix with untreated rubber (referred to as REF), the mix with rubber pre-treated by saturated sodium hydroxide solution for 2 h (CCSR20-N2h), the mix with rubber pre-treated by saturated sodium hydroxide solution for 24 h (CCSR20-N24h) and the mix with rubber pre-treated by SCA (CCSR20-SCA). Up to 20% by volume of the sand was replaced with CSR, and 50% by mass of the natural gravels was replaced with recycled aggregate in each mix. The mass ratio of water: binder: sand: natural gravel: recycled aggregate: rubber under the SSD condition is 0.37: 1: 0.66: 0.80: 0.80: 0.064 and all parameters were kept constant throughout the entire experimental programme.

Casting and Curing

The required quantity of each item was accurately measured out and placed in a mechanical mixer, which had been wetted on the internal surface. Before adding the water, the dry materials were blended for 5 min to produce an even distribution. The mixer was then allowed to run after the addition of water for several minutes until there were no visual discrepancies. All of the moulds used, including cube, cylinders and prisms, complied with BS EN 12390-1: 2012 (BSI, 2012). Prior to moulding, the moulds were treated with oil to allow smooth specimen faces and free removal of the moulds when de-moulding. All moulds were then filled with fresh concrete in two equal layers, each of which was compacted by using a vibration table. The exposed surface was trowelled off to a clean finish, after which polythene sheets were placed over the samples to prevent moisture loss and early cracking; they were then left for 24 h in the laboratory. After 24 h, the samples were carefully de-moulded and then transferred to a curing water tank where they were immersed in water at room temperature until they were tested.

Testing

To evaluate the workability of fresh concrete, slump tests were carried out in accordance with BS EN 12350-2 (BSI, 2009a). For hardened concrete, cube, prism and cylinder

specimens were used to determine the cube compressive strength, flexural strength and Young's modulus in accordance with BS EN 12390-3 (BSI, 2009b), 12930-5 (BSI, 2009c) and 12930-13 (BSI, 2013), respectively. The water permeability index was evaluated to assess the water resistance of each mix. An X-ray diffraction (XRD) test was carried out to analyse the crystals and phases of the composites. Scanning optical microscopy (SOM) was performed to observe the interface between the rubber and the matrix. Finally, the mercury intrusion method was adopted to characterise the pore structures of concrete with various surface-modified crumb rubber particles.

Results and discussion

Rubber surface

Crumb rubber particles were observed by SOM as shown in Figure 3. A micrograph of the untreated rubber surface (Figure 3(a)) shows that the particle has a rough surface with irregular dents and cracks, which were caused during the cutting and grinding of waste tyres. Figures 3(b) and 3(c) show that, apart from some sodium hydroxide crystals which are loosely attached to the surface of rubber particles, no significant visual differences in the rubber particle surfaces were found compared to untreated rubber. This indicates that sodium hydroxide treatment does not markedly alter the surface roughness of the rubber particles. Regarding the SCA-treated rubber, it is quite clear from the micro-image (Figure 3(d)) that a coating of gel-like silicone was found on the surface of the rubber particles. A hydrolysis reaction, which is the chemical characteristic of SCA and the primary mechanism of the coupling effect, happens when SCA encounters water. The product of the hydrolysis reaction is silanol, which can not only polymerise with hydroxyls of inorganic material, but can also self-polymerise, generating the silane polymer – silicones (Xanthos, 2005).

Workability

All the concrete mixtures were observed (by visual inspection) to be cohesive with no segregation during the mixing, placing or compaction. Figure 4 shows the slump for all four concrete mixes. A slump of 66 mm was recorded for the REF. The slump for the CCSR20-N2h, CCSR20-N24h and CCSR20-SCA concrete mixes is 4.5% (3 mm) higher, 3.0% (2 mm) higher and 13.6% (9 mm) lower than the REF mix, respectively. This result indicates that the pre-treatment with saturated sodium hydroxide solution affects the workability of concrete very slightly, as the slumps with and without pre-treated rubber are quite similar. In contrast, the pre-treatment with SCA decreased the workability noticeably. This is mainly ascribed to the sticky nature of an SCA-treated rubber surface, which tends to bond the rubber particles with the matrix, thus making the overall concrete mixture less workable. SCA is an organosilicon compound containing two different reactive groups. One functional group is organophilic, whereas the other polymerises and reacts with the surface of inorganic material. The formula of SCA is YSi(OR)3, where Y is a non-hydrolytic group which tends to bond well the synthetic resin, rubber, and so on, in organic materials; OR is a hydrolysable group that will hydrolyse in water to generate a silanol (Si–O–H) group) which will chemically react with hydroxyl on the surface of inorganic materials (such as silicate) to form a hydrogen bond. A further condensation reaction (dehydration synthesis) will then take place to form an oxygen covalent bond, and finally the surface of the inorganic material will be covered by the reaction products, thereby enhancing the cohesiveness (Xanthos, 2005). The reaction process is shown in Figure 5. Because of the special molecular structure of SCA, which can react with both organic and inorganic materials to form chemical bonds, two kinds of materials with different types of chemical structures can be well connected on their interface, thus decreasing the workability. In practical production, this can be easily corrected by adding a commonly available admixture such as a superplasticiser.

Strength and Young's modulus

Compressive strength tests for different mixes were carried out at 1 d, 7 d and 28 d. The results are shown in Figure 6. The 1-d compressive strengths of CCSR20-N2h and CCSR20-N24h were 2.4% (0.2 MPa) lower and 1.2% (0.1 MPa) higher than REF, respectively. However, the value of CCSR20-SCA was 1.6 MPa, which is 19.3% higher than that of REF. The 7-d compressive strengths of CCSR20-N2h, CCSR20-N24h and CCSR20-SCA were 5.2% (1 MPa) lower, 2.6% (0.5 MPa) higher and 9.3% (1.8 MPa) higher than REF, respectively. The 28-d compressive strengths of CCSR20-N2h, CCSR20-N24h and CCSR20-SCA were 2.2% (0.8 MPa) lower, 0.8% (0.3 MPa) higher and 6.8% (2.5 MPa) higher than REF, respectively. These results indicate that the improvement in compressive strength of the mixes containing sodium hydroxide pre-treated (2 h and 24 h) rubber is modest compared to the mix with untreated rubber. It can be further deduced that the surface modification of rubber particles by SCA has a better effect on the compressive strength enhancement than that treated with saturated sodium hydroxide solution (less than 24 h). This conclusion is also applicable to the properties of the Young's modulus and the flexural strength. The Young's moduli of REF, CCSR20-N2h and CCSR20-N24h were 22.1, 22.3 and 22.4 GPa, respectively, as shown in Figure 7. The difference between them is rather modest. The result of CCSR20- SCA in terms of the Young's modulus was 23.8 GPa, which is 7.7% higher than that of REF. Figure 8 shows the results of the flexural strength at 28 d for the different mixes. 4.6, 4.6, 4.6 and 4.7 MPa were recorded for the REF, CCSR20-N2h, CCSR20-N24h and CCSR20-SCA mixes, respectively. As compared to the reference mix, there was no difference for CCSR20-N2h and CCSR20-N24h. The increase for the CCSR20-SCA mix was 2.2%, which is not significant.

The above conclusions were supported by the microscopic inspections and analysis of the crushed sample particles at 28 d. The rubber–matrix interface was inspected by SOM, which was performed using a Keyence VHX-700F series optical microscope, shown in Figure 9. Detailed investigations on ten rubber particles of each specimen were performed.

Micrographs of typical fracture surfaces are shown in Figures 10–12. As shown in Figure 10(a), it is quite clear that there is a distinct crack highlighted by the curve in zone I. From the three-dimensional (3D) image (Figure 10(b)), significant discontinuity in zone II was found. Faults and cracks observed at the rubber–matrix interface indicate that the untreated rubber–concrete matrix adhesion is poor. Similar phenomena are also found in concrete samples CCSR20-N2h and CCSR20-N24h, as shown in Figure 11. No obvious difference was revealed after the rubber was treated with sodium hydroxide. The modest effect of sodium hydroxide treatment may be attributed to the limited roughness gained from the surface treatment of rubber particles by being soaked in saturated sodium hydroxide solution for less than 24 h. From the micrograph of CCSR20-N24h (Figure 11(b)), it can be seen that two cracks initialised from the surface of the rubber particle. This may be ascribed to the fact that the stiffness of rubber is low compared to the mineral aggregates. Rubber particles can be deemed as voids, and stress concentration usually arises at the interface between a rubber particle and the matrix. In the micrograph of CCSR20-SCA (Figure 12(a)), a well-developed adhesive joint area is observed between the SCA-treated rubber particles and the matrix, where the adhesion promoter has diffused to both substrate materials. From its 3D image shown in Figure 12(b), it can be seen that the transition zone between the rubber particle and the concrete matrix is very smooth, in contrast to the counterpart of REF as shown in Figure 10(b), where a clear trough can be observed in zone II. The observation for the CCSR20-SCA specimen suggests that there is a relatively stronger bond at the interface. The mechanism of this increase in bond strength, as illustrated above, is that the nature of SCA plays an enhanced role in developing bonding between organic and inorganic materials, leading to the improvements in compressive and flexural strengths.

X-ray diffraction analyses for the REF, CCSR20-N2h, CCSR20- N24h and CCSR20-SCA mixes were also carried out. A crushed sample particle was placed in a rubber container, which was then filled with liquid resin. After solidification, the sample was demoulded and ground until the surface of the concrete particle could be tested by X-ray (Figure 13). The

device used for this test was a D8 Discover from Bruker Corporation, as shown in Figure 14, with the test results shown in Figure 15. The diffraction pattern reveals a very intense diffraction peak A at around 278, which means that the major crystalline phase was quartz (SiO2). Another major crystalline phase was calcite (CaCO3), which was identified from the analysis of diffraction peak B. Apart from these two primary phases, the formation of germanium iron (Fe3Ge), and gismondine (CaAl2Si2O8 . 4H2O) was observed, as well as a small quantity of sabinaite (Na4Zr2-TiO4(CO3)4), tacharanite (Ca12Al2Si18O51 . 18H2O) and retgersite (NiSO4 . 6H2O). The angles and intensities of the diffraction peaks of the four samples are quite similar to each other, indicating hardly any difference, which means that the compositions are almost the same among these four samples. In other words, the pre-treatment by sodium hydroxide solution or by SCA does not change the phase constitution of rubber concrete significantly.

Water permeability

A water permeability test was performed using the Autoclam test equipment shown in Figure 16. The test was performed as a modified version of the initial surface absorption test (ISAT). 100 mm cube specimens were preconditioned (by being sheltered for 1 week) before the water permeability test was undertaken. The cumulative flow of water into the concrete cube at a pressure of 500 mbar was recorded every minute for 15 min. Figure 17 shows the volume of water flowing plotted against the square root of time, in accordance with the recommendations of The Concrete Society (2008). A regression equation for each specimen can be determined, and the gradient of the line between the fifth and the 15^{th} reading is known as the water permeability index. From the results of the graph, it was found that the water permeability indices of REF, CCSR20-N2h, CCSR20-N24h and CCSR20-SCA were 2.51, 2.43, 2.41 and 2.18 $m^3 \times 10^{-7} / \sqrt{min}$, respectively. The indices of the CCSR20-N2h and CCSR20-N24h mixes were approximately 96.4% of the reference mix, while that of CCSR20-SCA was 86.9%. This means that the surface modified rubber will improve the water permeability resistance compared to the as-received rubber. However, the effect of

sodium-hydroxide-treated rubber (for less than 24 h) is not as significant as SCA-treated rubber. The pre-treatment by SCA improves the adhesion between the rubber and the matrix and hence reduces the void or micro-crack size, and consequently reduces the micro-conduits through which water can penetrate.

The above phenomenalistic observations are supported by the results of the mercury intrusion porosimetry (MIP) test. The device used is AutoPore IV 9500 from Micromeritics Instrument Corporation, shown in Figure 18. Table 2 shows the porosity and tortuosity of the different mixes. The porosity of CCSR20-SCA was the lowest one, which was 6.5% less than REF. CCSR20-N2h and CCSR20-N24h were 4.3% and 3.9% lower than REF, respectively. The difference between CCSR20-N2h and CCSR20-N24h was insignificant. The values of tortuosity for CCSR20-N2h and CCSR20-N24h were 4 and 10 higher than REF, respectively. The value of CCSR20-SCA was the highest, and this was 47 higher than REF. This can be explained by the effect of SCA, causing the bonding between the rubber particles and the concrete matrix to be enhanced. The concrete mixture of CCSR20-SCA was denser than REF, leading to the lower porosity. Besides, because the conduits through which water can flow were reduced, water needs to find a longer path to travel from one pore to another, which means that the water permeability resistance was improved. Figures 19 and 20 show the pore size distribution of the different mixes. It can be seen that the four mixes have a similar trend in terms of pore size distribution. The range of the pore size is from 6 nm to 5×10^4 nm, with most being between 6 nm and 11 nm. The volume of intruded mercury increased sharply when the pore size was below 100 nm for each mix. It is quite clear from Figure 20 that when the pore diameter is greater than 11 nm, the mercury intrusion of the four samples is almost the same. When the pore diameter is around 7 nm or 9 nm, the mercury intrusion of REF is much higher than that of the other three samples. CCSR20-N2h and CCSR20-N24h are much closer to each other in terms of mercury intrusion. CCSR20-SCA shows the lowest volume of intruded mercury in general, which

confirms that it has the lowest porosity, leading to the best water permeability resistance of the four mixes.

Cost analysis

The price of rubber crumb used in this study is £240/t, higher than the price of natural river sand which is around £35/t. However, based on the mix design, if 20% of natural river sand is replaced by rubber crumbs by volume, a batch of 24 m^3 of rubber concrete roughly needs 1 tonne of rubber crumb. The price ratio of crumb rubber to concrete can be calculated as £240/(£100/m^3 × 24 m^3), equal to 1/10. So the cost of rubber accounts for approximately one tenth of the total resulting cost, which is rather limited.

The price of chemically pure SCA and solid sodium hydroxide powders is about £20/kg and £2/kg, respectively. Chemically pure SCA needs to be diluted to 1% of mass fraction before using it to treat crumb rubber. The solid sodium hydroxide powder is dissolved in water to prepare saturated sodium hydroxide solution. Solubility of sodium hydroxide under laboratory temperature 208C is 109 g/(100 g water). Table 3 shows the details on the capital cost. It can be found that the cost of SCA solution is around £8 per cubic metre of concrete, which is much cheaper than the cost of sodium hydroxide solution, namely, £44 per cubic concrete. In practice, the solution can be reused many times. Therefore, the extra cost of the treatment solution is reasonably low. Besides, tax is levied on the disposal of waste tyres. The tax expense saved by reusing the waste tyres can almost offset the additional costs introduced by the crumb rubber and its surface treatment, which makes this application economically viable.

In addition, a more important sustainability credential for rubber concrete using waste tyres lies in the environmental aspect, not only through reducing the production of wastes but also by alleviating the pressure of diminishing natural resources. The improved performance of the resulting concrete, such as enhanced ductility and energy absorption, is another positive driver for utilising this type of concrete.

Conclusions

In this study, the effects of rubber surface modifications by saturated sodium hydroxide solution and SCA on the concrete properties such as workability, compressive strength, flexural strength, Young's modulus and water permeability, were investigated. The main findings include that the surface-modified rubber pre-treated with SCA has a more positive effect on the concrete properties than that treated with saturated sodium hydroxide solution. Pre-treatment with saturated sodium hydroxide solution for less than 24 h does not produce significant changes in the properties of concrete compared to concrete containing as received rubber. However, in contrast to the control mix, the pre-treatment with SCA, which acts as an adhesion promoter, enhances the adhesion of tyre rubber particles to the matrix, resulting in

(a) a reduction in the slump values of fresh concrete by 13.6%

(b) an improvement in the compressive strength of hardened concrete by 19.3% at 1 d, 9.3% at 7 d and 6.8% at 28 d

(c) an increase in the Young's modulus of hardened concrete by 7.7% at 28 d

(d) an improvement in the flexural strength of hardened concrete by 2.2% at 28 d

(e) a decrease of the water permeability index of hardened concrete by 13.1%.

The SOM inspection of test specimens showed that the rubber–matrix adhesion will be enhanced with the use of SCA. The XRD data of the different mixes showed similar diffraction patterns, which means that pre-treatment by saturated sodium hydroxide solution or by SCA does not change the crystalline phase of rubber concrete significantly. The MIP test showed that concrete with SCA-treated rubber has a similar pore size distribution to the control mix and to the concrete with sodium-hydroxidetreated rubber, but it achieves the lowest porosity and the highest tortuosity, which will result in the best water permeability resistance. A brief cost analysis was also carried out, demonstrating the economic viability of this type of rubber concrete that reuses waste tyres. This feature, together with the well-

accepted attractiveness in terms of sustainability and technical benefits, reinforces the potential prospects of this concrete material.

Acknowledgements

Some contents of this paper were presented as a poster in the Young Researchers Forum II organised by the Institute of Concrete Technology in University College London, UK. The financial support of the Institution of Structural Engineers (IStructE) to this project is gratefully acknowledged. The second author would also like to acknowledge funding from the Shanghai Pujiang Program, People's Republic of China (13PJ1405200).

References

Aiello M and Leuzzi F (2010) Waste tyre rubberized concrete: properties at fresh and hardened state. *Waste Management* **30(8–9):** 1696–1704.

Albano C, Camacho N, Reyes J et al. (2005) Influence of scrap rubber addition to Portland I concrete composites: destructive and non-destructive testing. *Composite Structures* **71(3–4):** 439–446.

Benazzouk A, Douzane O, Langlet T et al. (2007) Physico-mechanical properties and water absorption of cement composite containing shredded rubber wastes. *Cement and Concrete Composites* **29(10):** 732–740.

Bignozzi MC and Sandrolini F (2006) Tyre rubber waste recycling in self-compacting concrete. *Cement and Concrete Research* **36(4):** 735–739.

BSI (2009a) BS EN 12350-2 Testing fresh concrete – Part 2: Slump-test. BSI, London, UK.

BSI (2009b) BS EN 12390-3 Testing hardened concrete – Part 3: Compressive strength of test specimens. BSI, London, UK.

BSI (2009c) BS EN 12390-5 Testing hardened concrete – Part 5: Flexural strength of test specimens. BSI, London, UK.

BSI (2012) BS EN 12390-1 Testing hardened concrete. Shape, dimensions and other requirements for specimens and moulds. BSI, London, UK.

BSI (2013) BS EN 12390-13 Testing hardened concrete – Part 13: Determination of secant modulus of elasticity in compression. BSI, London, UK.

Eldin NN and Senouci AB (1993) Rubber-tire particles as concrete aggregate. *Journal of Materials in Civil Engineering* **5(4):** 478–496.

Ganjian E, Khorteza M and Maghsoudi AA (2009) Scrap-tyre-rubber replacement for aggregate and filler in concrete. *Construction and Building Materials* **23(5):** 1828–1836.

Gokce HS and Simsek O (2013) The effects of waste concrete properties on recycled aggregate concrete properties. *Magazine of Concrete Research* **65(14):** 844–854.

Guneyisi E, Gesoglu M and Ozturan T (2004) Properties of rubberized concretes containing silica fume. *Cement and Concrete Research* **34(12):** 2309–2317.

Hansen TC and Narud H (1983) Strength of recycled concrete made from crushed concrete coarse aggregate. *Concrete International: Design and Construction* **5(1):** 79–83.

Khaloo AR, Dehestani M and Rahmatabadi P (2008) Mechanical properties of concrete containing a high volume of tire-rubber particles. *Waste Management* **28(12):** 2472–2482.

Khatib ZK and Bayomy FM (1999) Rubberized Portland cement concrete. *Journal of Materials in Civil Engineering* **11(3):** 206–213.

Li G, Stubblefield MA, Garrick G et al. (2004) Development of waste tire modified concrete. *Cement and Concrete Research* **34(12):** 2283–2289.

Li J, Chen Z, Xie Wet al. (2009) Experimental study of recycled rubber-filled high-strength concrete. *Magazine of Concrete Research* **61(7):** 549–556.

Ling TC (2011) Prediction of density and compressive strength for rubberized concrete blocks. *Construction and Building Materials* **25(11):** 4303–4306.

Nehdi M and Khan A (2001) Cementitious composites containing recycled tire rubber: an overview of engineering properties and potential applications. *Cement Concrete and Aggregates* **23(1):** 3–10.

Poon CS, Shui ZH, Lam L et al. (2004) Influence of moisture states of natural and recycled aggregates on the slump and compressive strength of concrete. *Cement and Concrete Research* **34(1):** 31–36.

Prasad DSV, Prasada Raju GVR and Anjan Kumar M (2009) Utilization of industrial waste in flexible pavement construction. *Electronic Journal of Geotechnical Engineering* **13(1):** 12–12.

Raghavan D, Huynh H and Ferraris CF (1998) Workability, mechanical properties, and chemical stability of a recycled tyre rubber-filled cementitious composite. *Journal of Materials Science* **33(7):** 1745–1752.

Ravindrajah RS, Loo YH and Tam CT (2006) Strength evaluation of recycled aggregate concrete by in-situ tests. *Materials and Structures* **21(4):** 289–295.

Saravanakumar P and Dhinakaran G (2014) Durability aspects of HVFA-based recycled aggregate concrete. *Magazine of Concrete Research* **66(4):** 186–195.

Savas BZ, Ahmad S and Fedroff D (1997) Freeze–thaw durability of concrete with ground waste tire rubber. *Transportation Research Record* **1574:** 80–88.

Segre N and Joekes I (2000) Use of tire rubber particles as addition to cement paste. *Cement and Concrete Research* **30(9):** 1421–1425.

Siddique R and Naik TR (2004) Properties of concrete containing scrap-tire rubber – an overview. *Waste Management* **24(6):** 563–569.

Singh B, Sahoo DK and Jacob NM (2013) Efficiency factors of recycled aggregate concrete bottle-shaped struts. *Magazine of Concrete Research* **65(14):** 878–887.

Snelson DG, Kinuthia JM, Davies PA et al. (2009) Sustainable construction: composite use of tyres and ash in concrete. *Waste Management* **29(1):** 360–367.

Tantala MW, Lepore JA and Zandi I (1996) Quasi-elastic behaviour of rubber included concrete using waste rubber tyres. In *Proceedings of the 12th International Conference on Solid Waste Technology and Management, Philadelphia* (Zandi I (ed.)). University of Philadelphia Press, USA.

The Concrete Society (2008) *Permeability Testing of Site Concrete*. The Concrete Society, UK, Technical Report No. 31.

Topçu IB (1995) The properties of rubberized concretes. *Cement and Concrete Research* **25(2):** 304–310.

Topçu IB and Avcular N (1997) Collision behaviours of rubberized concrete. *Cement and Concrete Research* **27(12):** 1893–1898.

Toutanji HA (1995) The use of rubber tire particles in concrete to replace mineral aggregates. *Cement and Concrete Composites* **18(2):** 135–139.

Xanthos M (2005) *Functional Fillers for Plastics*. Wiley, Germany, pp. 59–83.

Yang L, Zhu H and Li C (2011a) Strength and flexural strain of CRC specimens at low temperature. *Construction and Building Materials* **25(2):** 906–910.

Yang J, Du Q and Bao YW (2011b) Concrete with recycled concrete aggregate and crushed clay bricks. *Construction and Building Materials* **25(4):** 1935–1945.

LIST OF TABLES

Table 1 SSD density and SSD water absorption of natural and rubber aggregates

Item	Sand	Crushed gravels	Recycled aggregate	CSR
SSD[a] density: kg/m^3	2512	2581	2539	973
SSD water absorption: %	1.37	1.26	7.09	8.46

[a]SSD indicates saturated surface dry.

Table 2 Porosity and tortuosity of different mixes

Notation	Porosity: %	Tortuosity
REF	20.5	116
CCSR20-N2h	16.2	120
CCSR20-N24h	16.6	126
CCSR20-SCA	14.0	163

Table 3 Cost of different treatment solutions

Item	Cost of chemically pure material: £/kg	Cost of solution: £/kg	Cost per unit concrete: £/m^3
SCA	20	0.20	8.54
Sodium hydroxide	2	1.04	44.41

LIST OF FIGURES

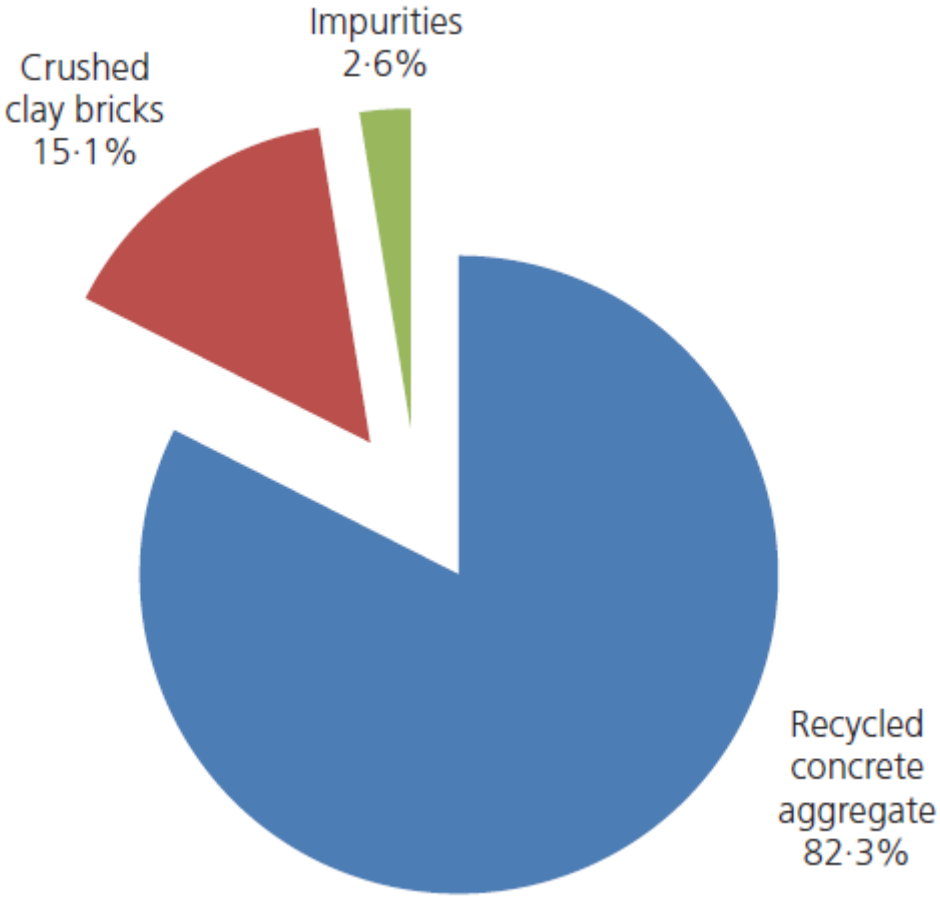

Figure 1 Composition of recycled aggregate

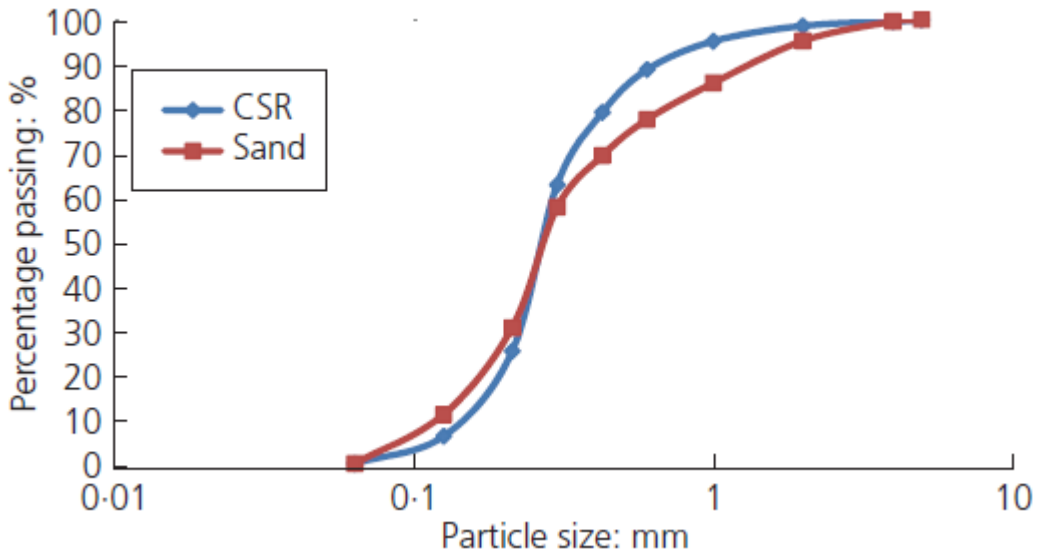

Figure 2 Grading curves of sand and rubber particles

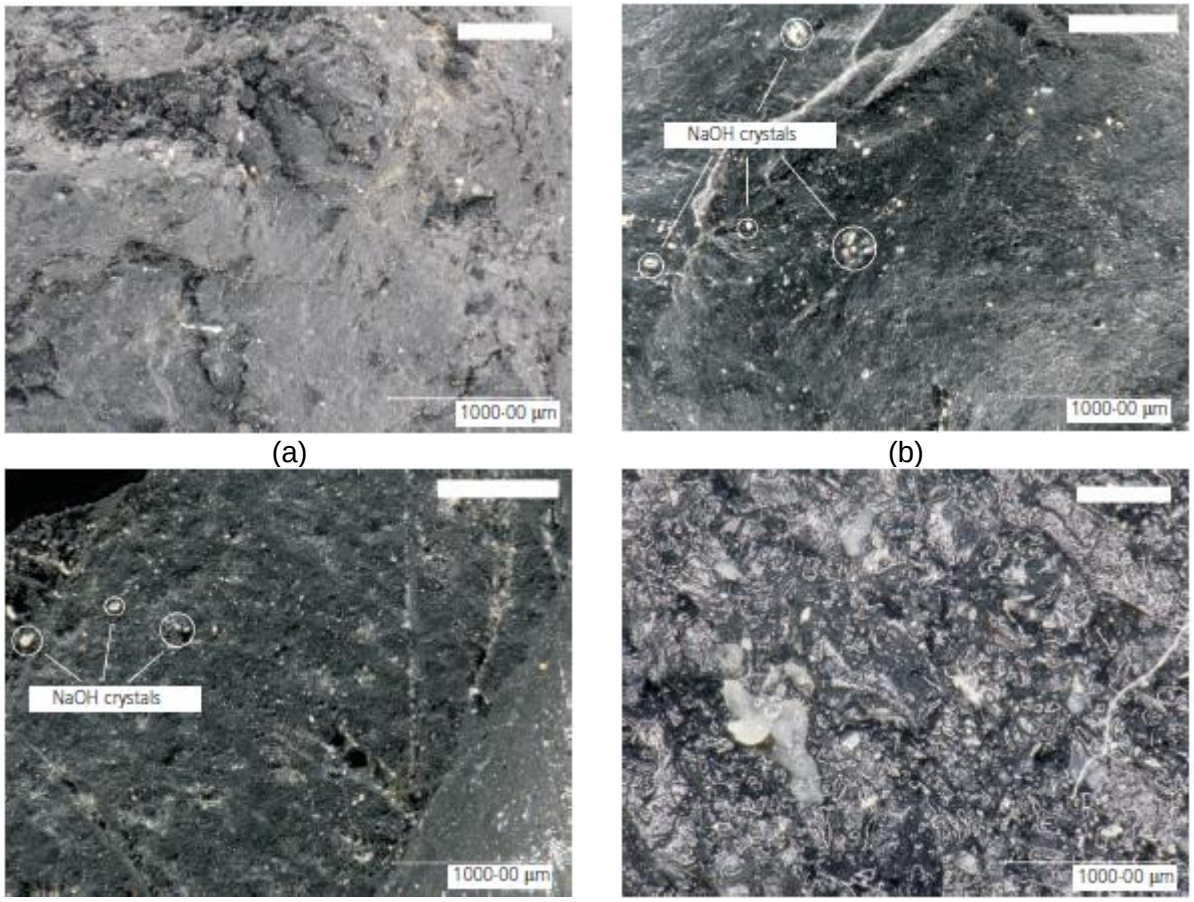

Figure 3 Micrographs of rubber particle surface: (a) untreated rubber surface; (b) sodium-hydroxide-treated rubber surface (2 h); (c) sodium-hydroxide-treated rubber surface (24 h); (d) SCA-treated rubber surface

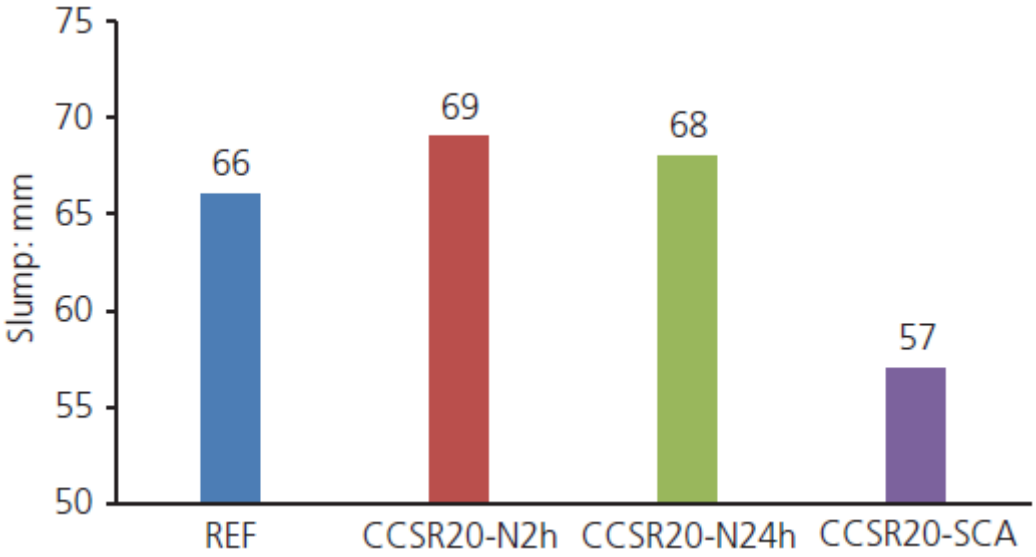

Figure 4 Slump test results of all the mixes

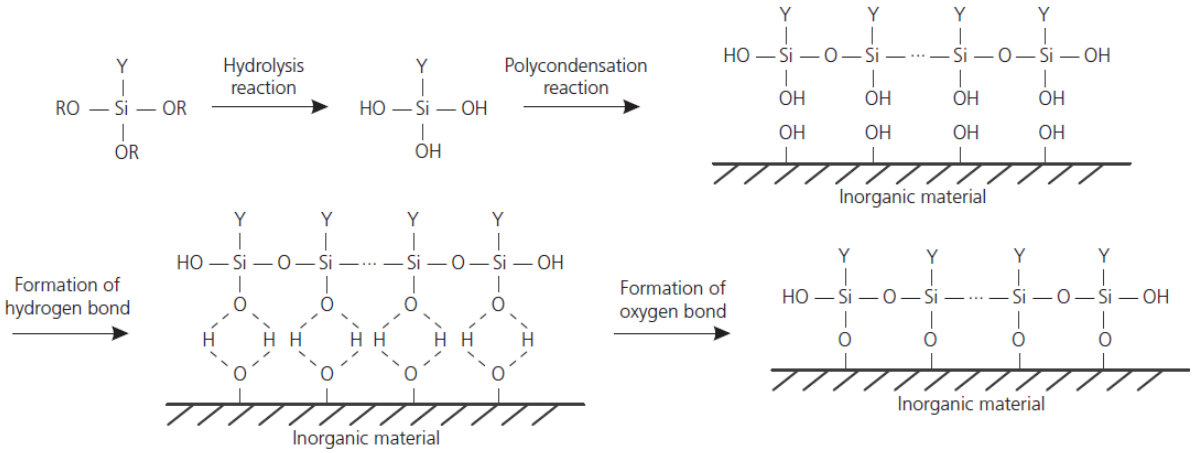

Figure 5 Reaction process of SCA with inorganic materials

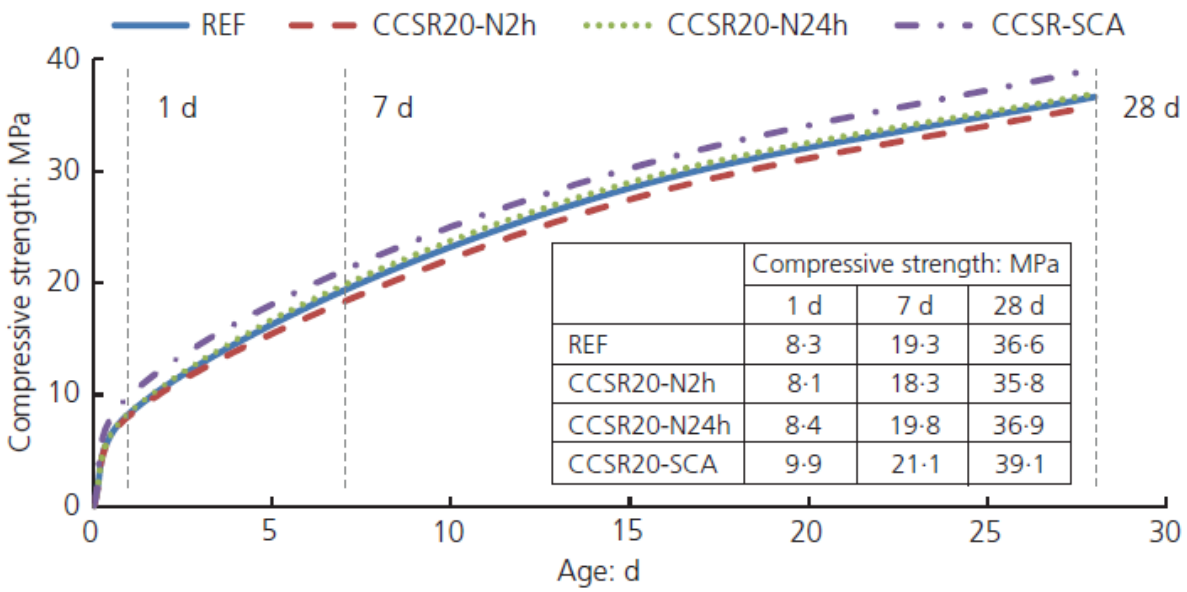

	Compressive strength: MPa		
	1 d	7 d	28 d
REF	8·3	19·3	36·6
CCSR20-N2h	8·1	18·3	35·8
CCSR20-N24h	8·4	19·8	36·9
CCSR20-SCA	9·9	21·1	39·1

Figure 6 Cube compressive strength test results of all mixes

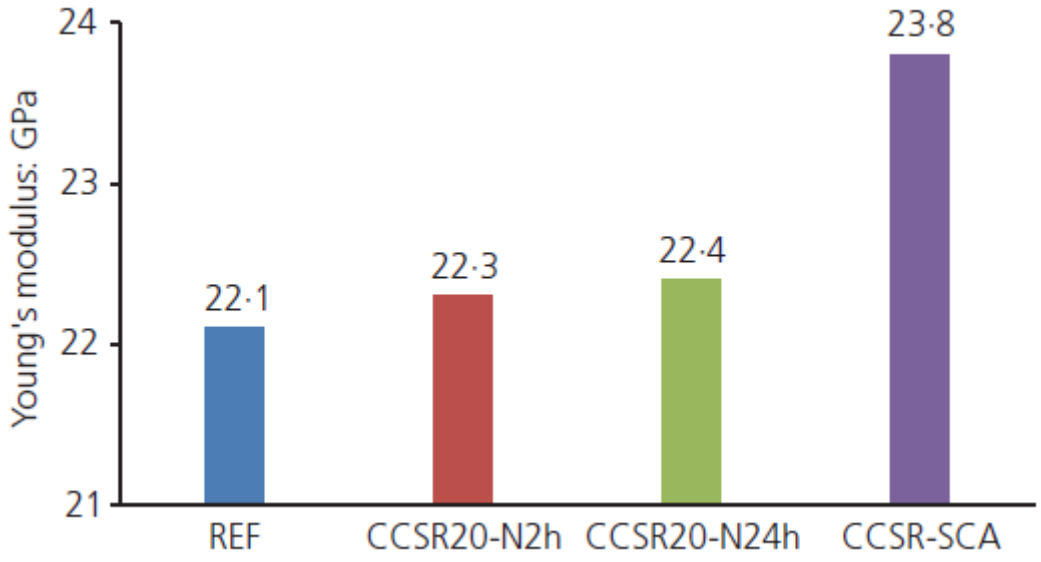

Figure 7 Young's modulus

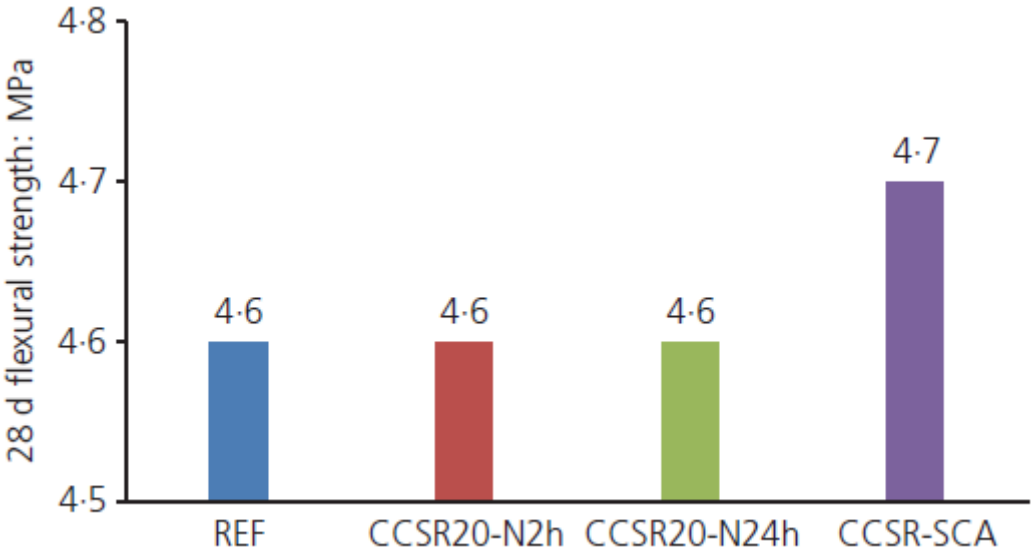

Figure 8 Flexural strength test results of all the mixes at 28 d

Figure 9 Keyence VHX-700F series optical microscope

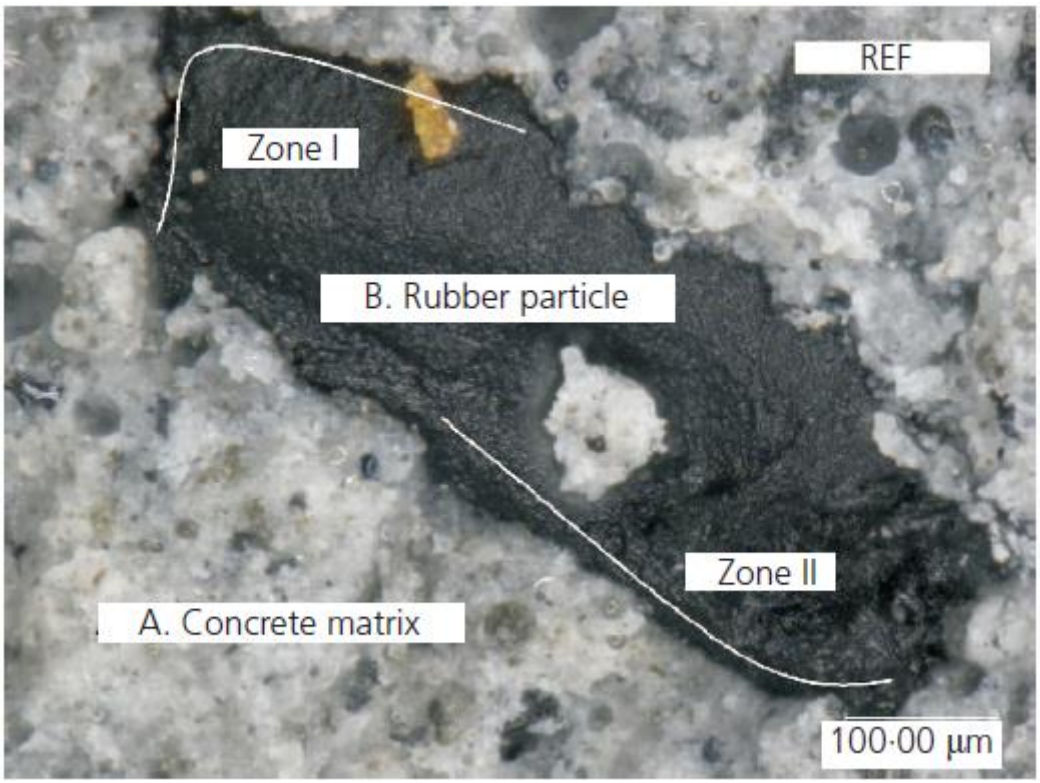

(a)

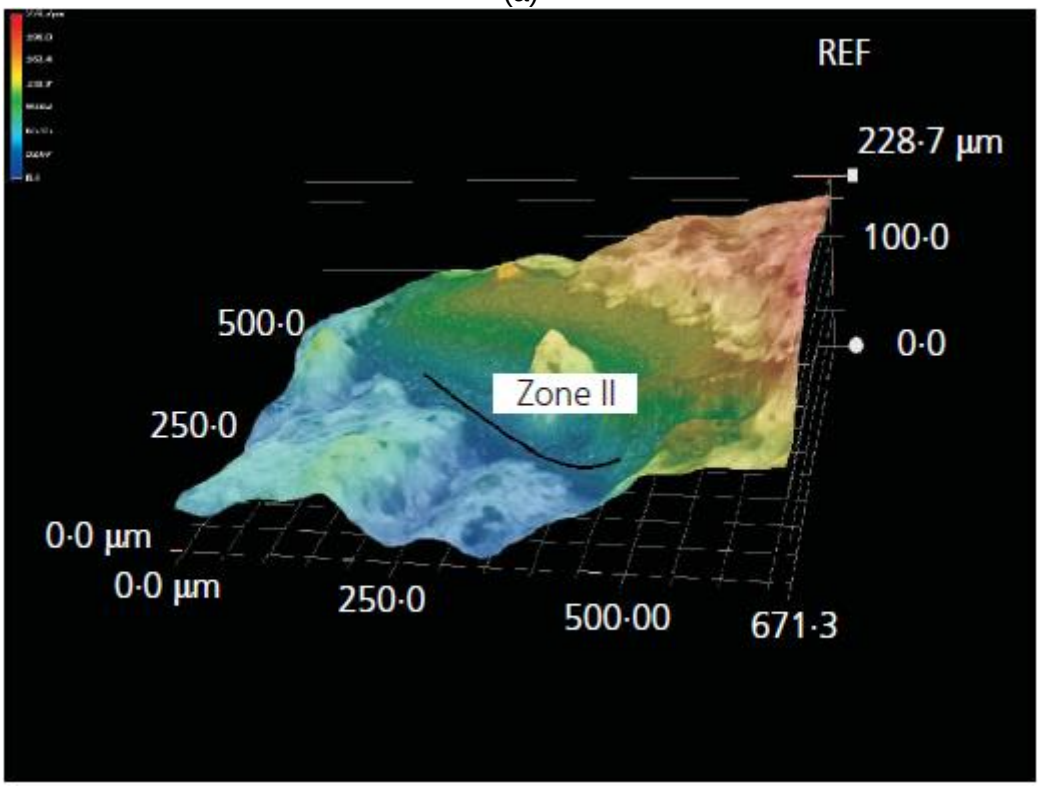

(b)

Figure 10 Rubber–matrix interface micrograph of: (a) REF and (b) its 3D image

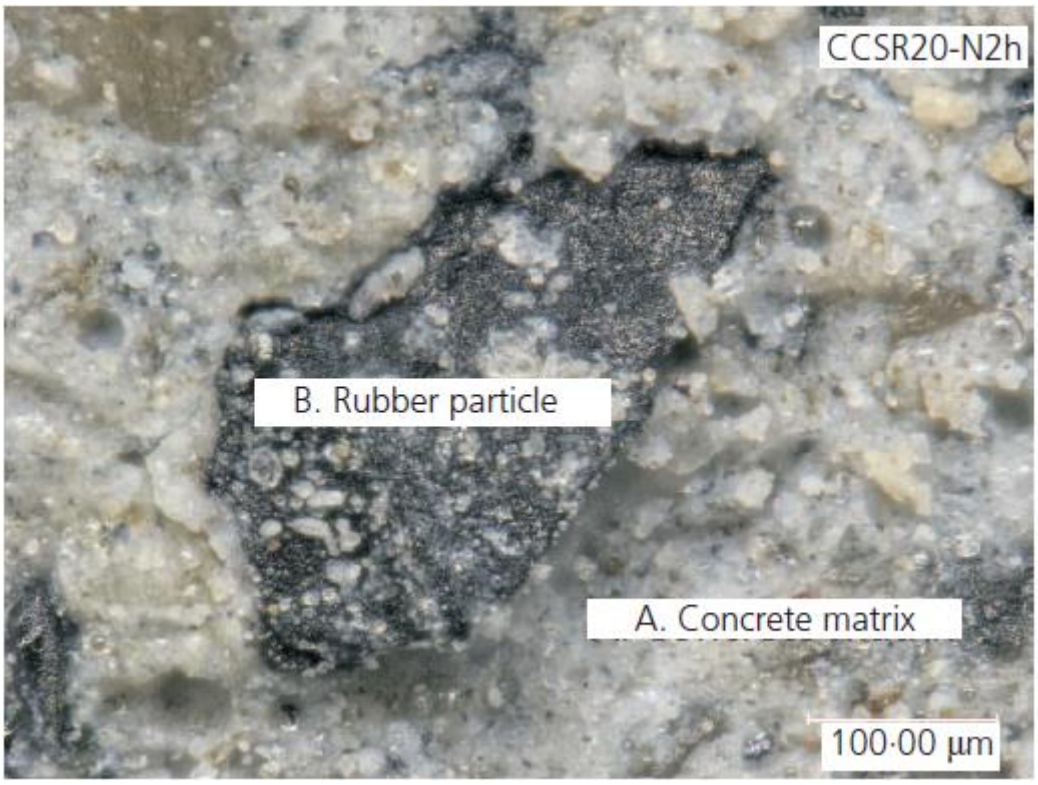

(a)

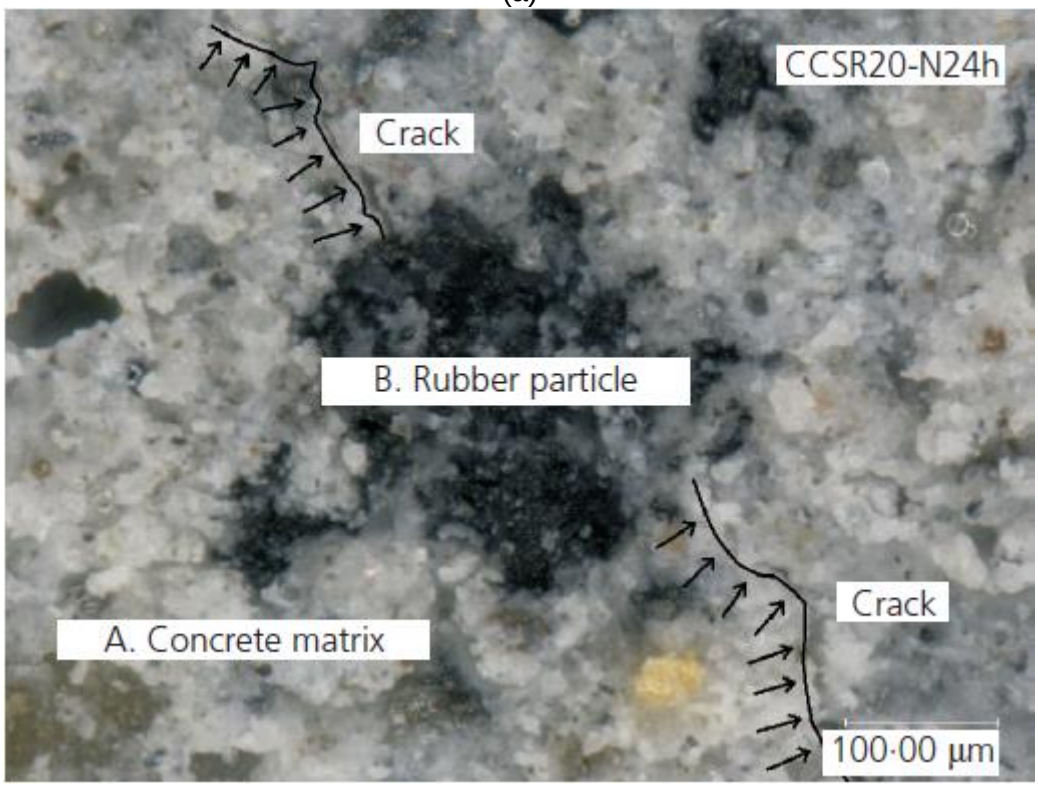

(b)

Figure 11 Rubber–matrix interface micrograph of: (a) CCSR20-N2h and (b) CCSR20-N24h

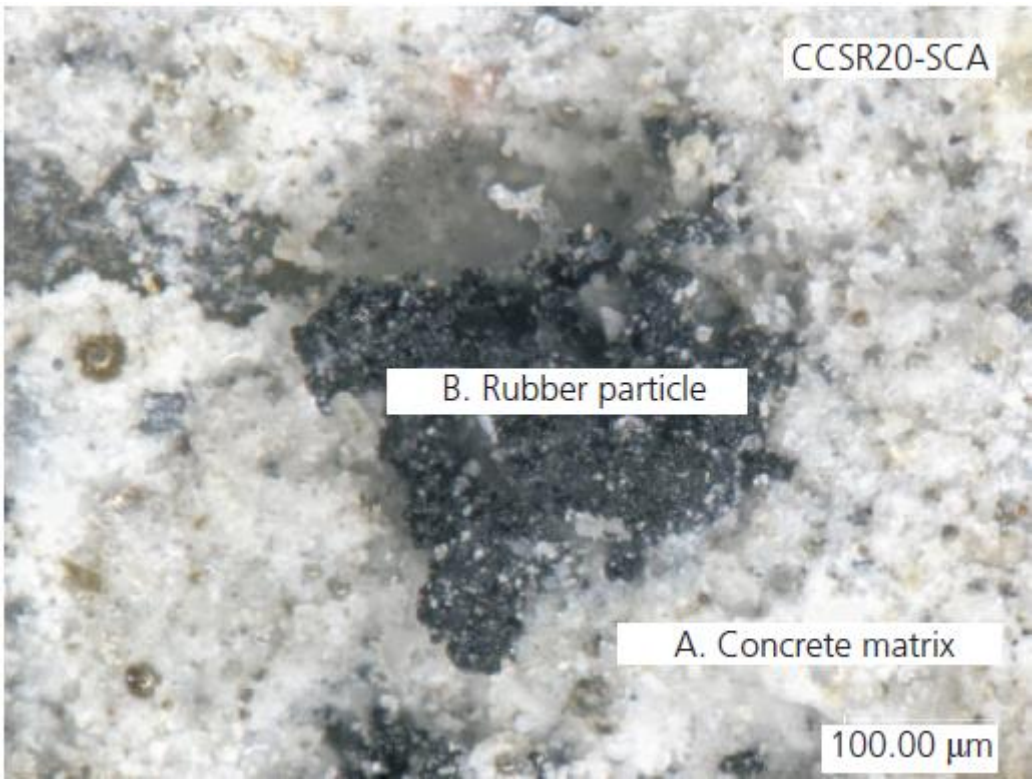

(a)

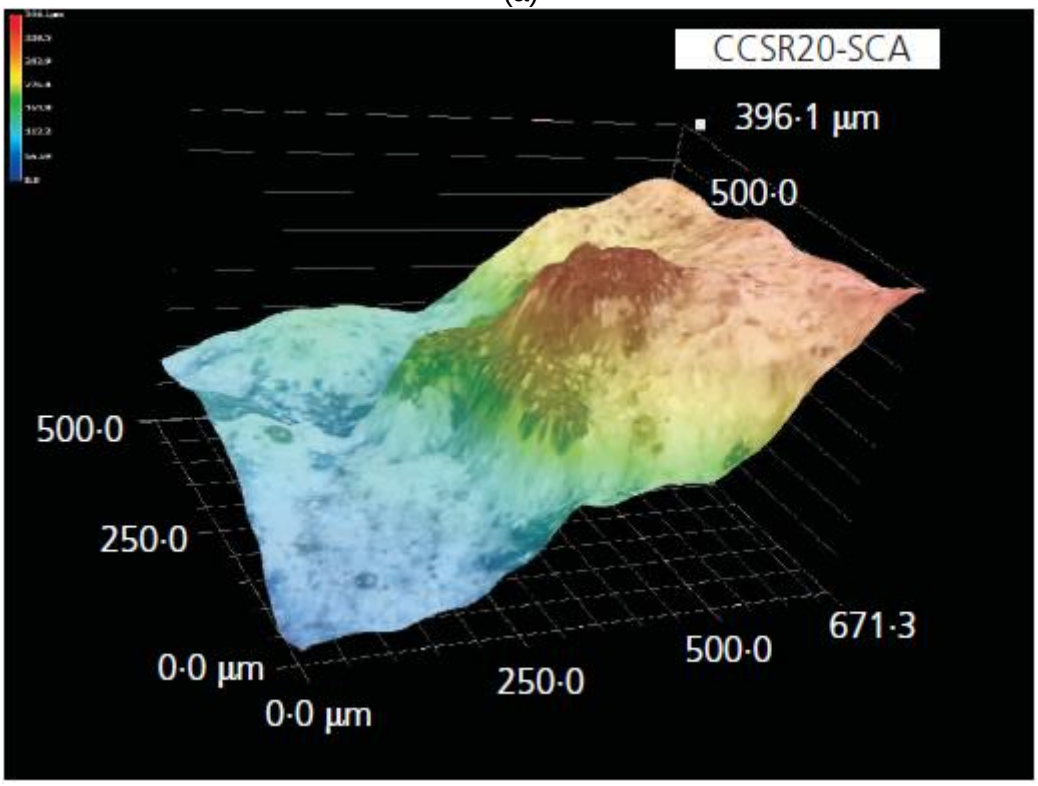

(b)

Figure 12 Rubber–matrix interface micrograph of: (a) (CCSR20-SCA) and (b) its 3D image

Figure 13 Concrete particle sample for XRD testing

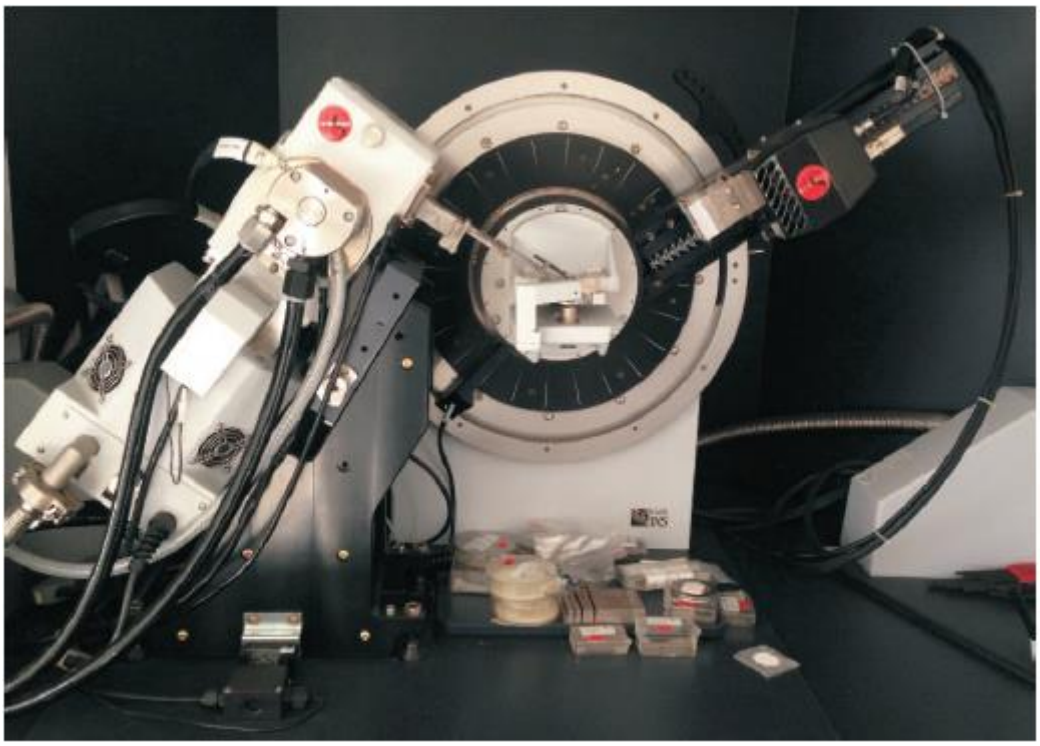

Figure 14 D8 Discover from Bruker Corporation

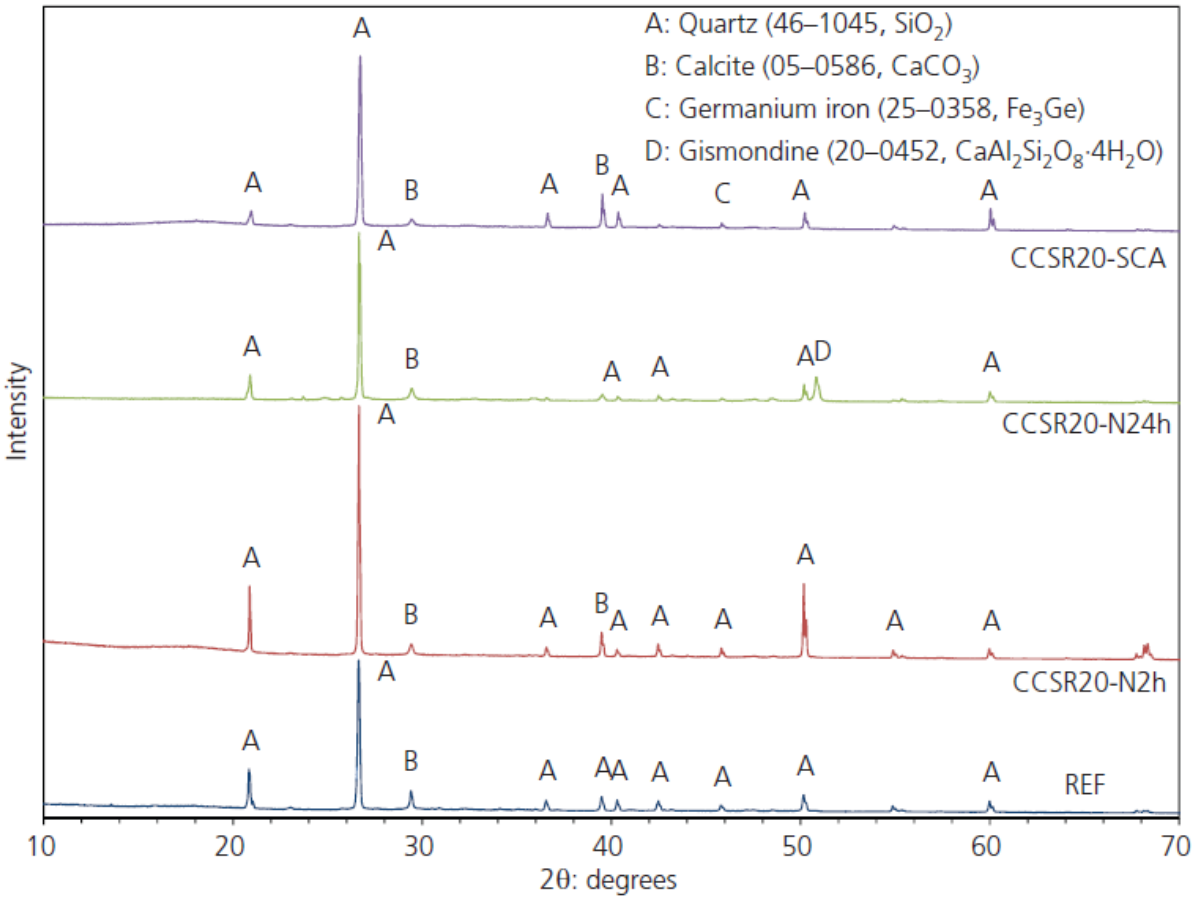

Figure 15 X-ray diffraction patterns of different samples

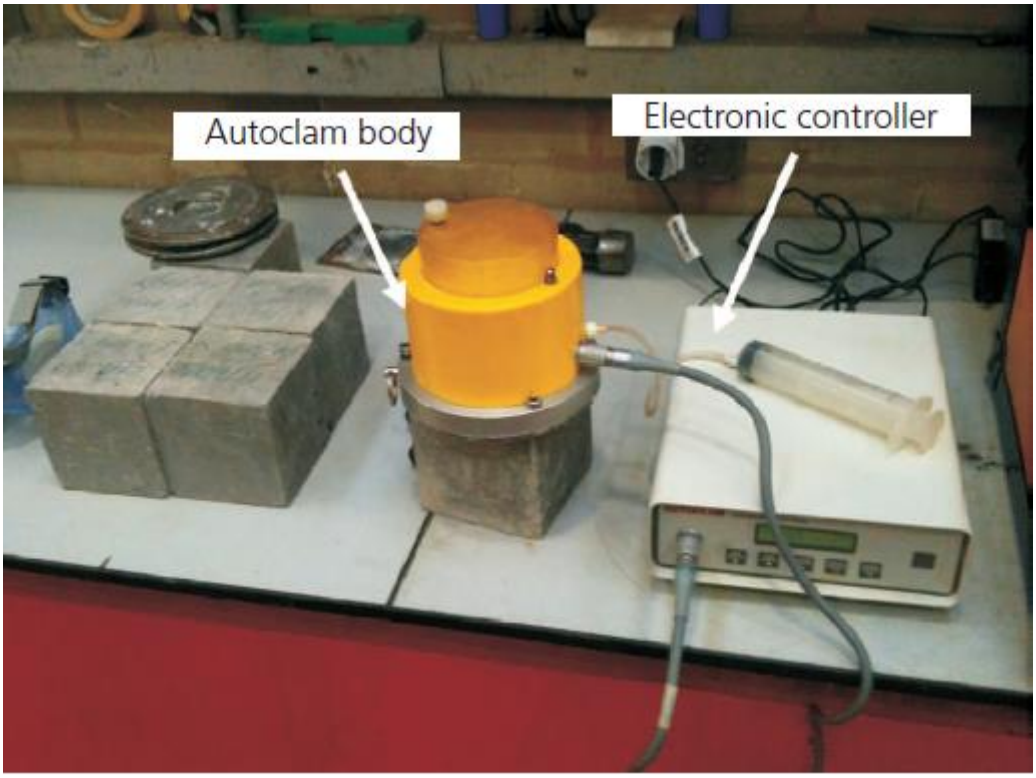

Figure 16 Apparatus for water permeability test

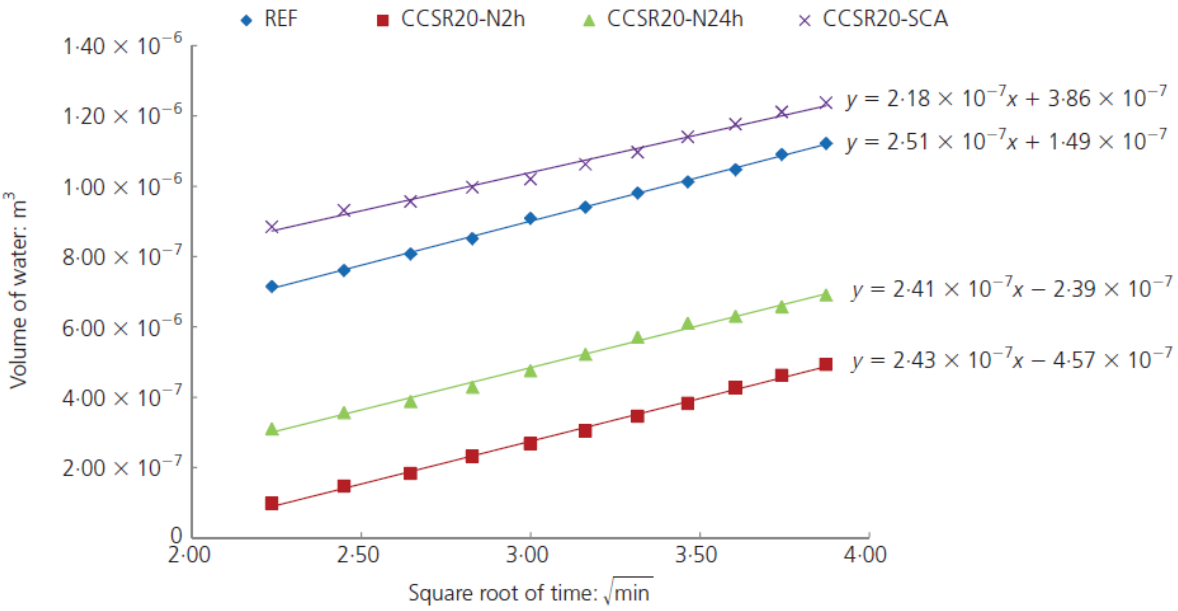

Figure 17 Volume of water flowing into specimen with time

Figure 18 AutoPore IV 9500 from Micromeritics Instrument Corporation

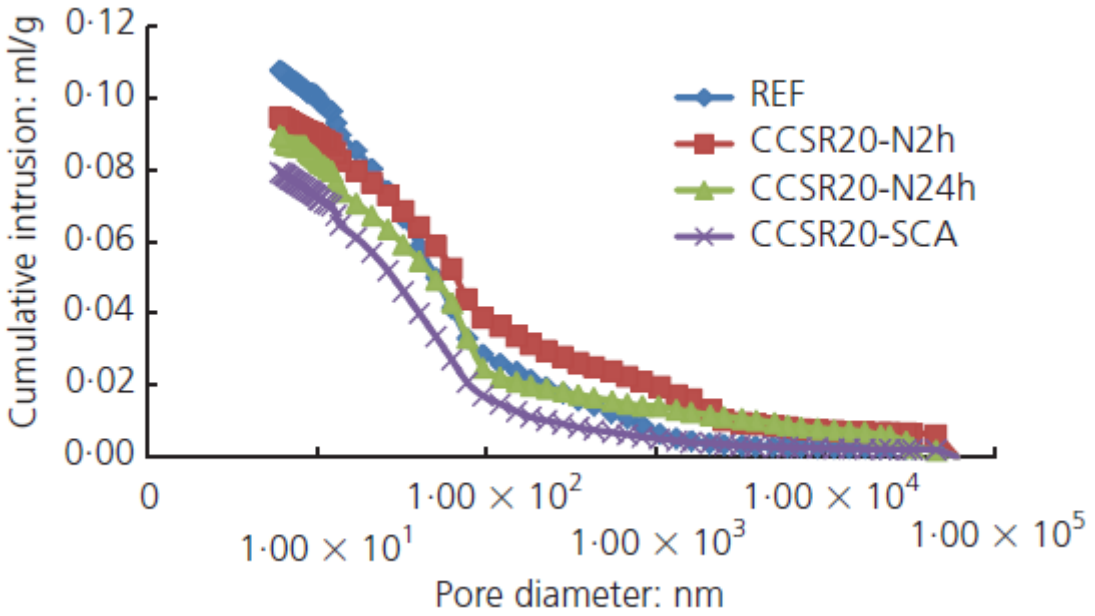

Figure 19 Pore size distribution of different mixes (cumulative intrusion against pore diameter)

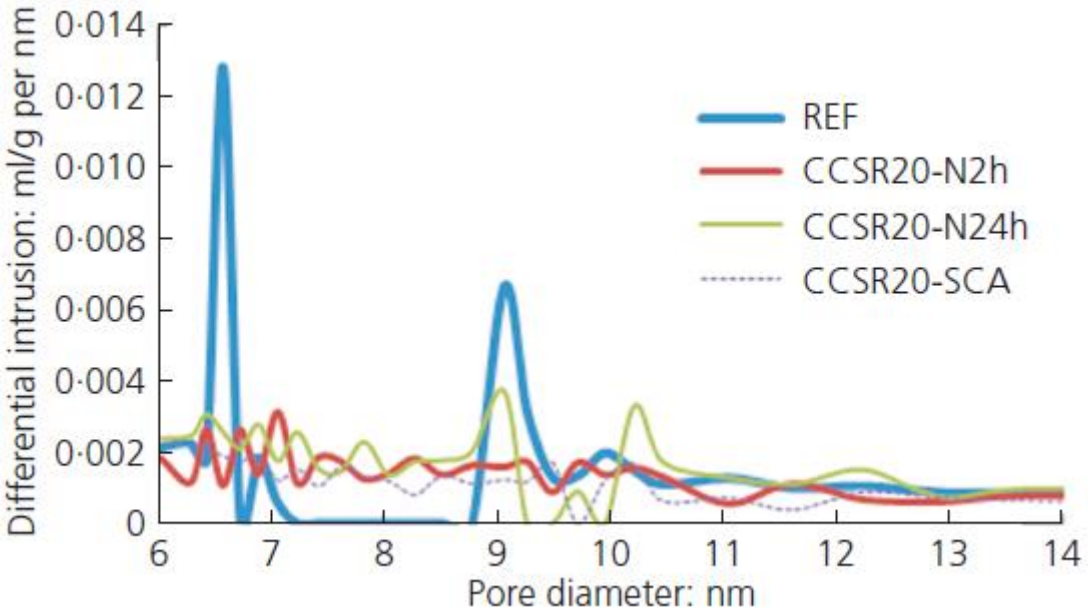

Figure 20 Pore size distribution of different mixes (differential intrusion against pore diameter)